Fabrication of Ni–W–P nanowire arrays by electroless deposition and magnetic studies

X.Y. Yuan[a,b,*], T. Xie[a], G.S. Wu[a], Y. Lin[a], G.W. Meng[a], L.D. Zhang[a]

[a]Institute of Solid State Physics, Chinese Academy of Sciences, P.O. Box 1129, Hefei 230031, PR China
[b]Department of Chemistry, Anhui University, Hefei 230039, PR China

Abstract

Ni–W–P alloy nanowire arrays have been fabricated by electroless deposition in an anodic alumina membrane. The images of Ni–W–P nanowire arrays and single nanowires are obtained by scanning electron microscope and transmission electron microscope, respectively. Selected area electron diffraction, X-ray diffraction (XRD) and energy dispersive spectra are employed to study the morphology and chemical composition of the nanowires. The results indicate that Ni–W–P nanowire arrays are amorphous in structure. The magnetic property of Ni–W–P alloy nanowire arrays is characterized using a vibrating sample magnetometer. The hysteresis loops show that the easily magnetized direction of Ni–W–P nanowire arrays is parallel to the nanowire arrays and that it has obvious magnetic anisotropy as a result of the shape anisotropy. Electroless deposition opens up significant opportunities in the nanoscale fabrication of magnetic materials for ultra-high-density magnetic recoding.
© 2004 Elsevier B.V. All rights reserved.

1. Introduction

The fabrication of magnetic nanowire arrays has become the subject of intensive study [1–4] due to their potential applications in ultra-high-density magnetic storage devices and microsensors [5]. Magnetic nanowire arrays as an ultra-high-density magnetic storage material can achieve recoding densities of more than 100 Gbit/inch^2, which is beyond the projected thermal limits of 40 Gbit/inch^2 in continuous magnetic film [6,7]. This kind of usage mainly takes advantage of the perpendicular anisotropy as a result of the shape anisotropy of nanowire arrays. But in some cases (such as Co, Ni nanowires), due to the competition between magnetocrystalline anisotropy and shape anisotropy, there may be no perpendicular anisotropy [8,9]. Since the magnetic properties of nanowire arrays are related to their element components and morphology, ternary alloy amorphous magnetic nanowire arrays are expected to exhibit the perpendicular anisotropy. An aim to be pursued is to fabricate perpendicular anisotropy ternary magnetic nanowire arrays for ultra-high-density magnetic recording. Although there have been reports of fabrication of single element and binary alloy

* Corresponding author. Institute of Solid State Physics, Chinese Academy of Sciences, P.O. Box 1129, Hefei 230031, PR China. Fax: +86-551-559-1434.

E-mail address: hfyxy@sohu.com (X.Y. Yuan).

magnetic nanowire arrays by electrodeposition in anodic alumina membrane (AAM) [10–14], ternary alloy magnetic nanowire arrays have not been reported so far. Because the redox evolution potential and thermodynamic stability of these elements are different, it is very difficult to electrodeposit large-scale and uniform ternary alloy nanowire arrays in an aqueous solution, especially in a solution containing such elements as tungsten (W) and phosphor (P). In fact, W is hardly electrodeposited from an aqueous solution, much less in its ternary alloy. Here, we have succeeded in fabricating large-scale and uniform Ni–W–P alloy nanowire arrays with electroless deposition in AAM. Compared with the electrodeposition method, electroless deposition method needs neither a supply of power nor a sprinkling of gold (Au, as a conductive layer) on one side of the AAM before the deposition, which is carried out via the redox reaction of an oxidizer and a reductant in an electrolyte solution. It is an autocatalytic self-assembly process, which is promising for the production of uniform nanowire arrays on a large-scale, and more importantly it will make it possible to finely control the aspect ratio of the nanowire using pores of different diameters and AAM thicknesses. Control of the uniform size and shape of nanowire arrays on a large-scale is recognized as a very important issue in the fabrication of nanostructure [15–17] and turned out to be a challenging problem [18–21]. In addition, electroless deposition method can be applied to many other materials [22] and open up significant opportunities in the nanoscale fabrication of magnetic material for ultra-high-density magnetic recoding.

2. Experimental

The AAM template was prepared just as described in Masuda and Fukuda [23]. The pores of the AAM template were about 60 nm in diameter and 15 μm in length with interpore spacing of 100 nm. The through-hole AAM template was first immersed in an aqueous solution of $SnCl_2$ (10 g l^{-1}) for 1 min and washed with distilled water 2–3 times, and then, the AAM template was further kept in a solution of $PdCl_2$ (1 g l^{-1}) for 30 s and

rinsed with distilled water several times again. Subsequently, Ni–W–P nanowire arrays were deposited in the pores of the AAM from a solution of 15 g l^{-1} $NiSO_4 \cdot 6H_2O$, 10 g l^{-1} $Na_2WO_4 \cdot 2H_2O$, 22 g l^{-1} $NaH_2PO_2 \cdot H_2O$, and 40 g l^{-1} sodium citrate at 80–85°C.

In order to isolate the Ni–W–P nanowire arrays, the AAM with Ni–W–P nanowire arrays was dissolved in 5 wt% NaOH solution at 25°C for 5 min and slightly washed several times with distilled water to remove the dissolved AAM and the remaining NaOH solution. For scanning electron microscope (SEM, JSM-6700F) images, the above Ni–W–P nanowire arrays were directly mounted on Cu stubs with a conductive gold paint. The sample for the transmission electron microscope (TEM, H-800) was treated with a 5 wt% NaOH solution for 10 min and dispersed in alcohol. Then a small drop of the solution was placed on a carbon film supported by Cu grids.

Selected area electron diffraction (SAED), energy dispersive spectra (EDS, TEM JEOL-2010) and X-ray diffraction (XRD, MXP18AHF) were employed to study the chemical composition and morphology of the nanowires. The magnetic property of Ni–W–P alloy nanowire arrays was characterized using a vibrating sample magnetometer (VSM, BHV-55), with the applied magnetic field parallel or perpendicular to nanowire arrays.

3. Results and discussion

Fig. 1 shows a SEM image of Ni–W–P alloy nanowire arrays prepared by electroless deposition in an AAM. Fig. 1a shows the view from the top and Fig. 1b shows the view from the side. Fig. 1a indicates that the Ni–W–P alloy nanowire arrays are uniform in size and all pores of the AAM are filled up. Fig. 1b reveals that the nanowires are parallel to each other and the nanowires are about 3 μm in length. The SEM images reveal that the Ni–W–P nanowire arrays fabricated by electroless deposition are large-scale uniform in size and shape. The reactions in the fabrication of Ni–W–P nanowire arrays are as follows:

$$SnCl_2 + PdCl_2 = SnCl_4 + Pd, \qquad (1)$$

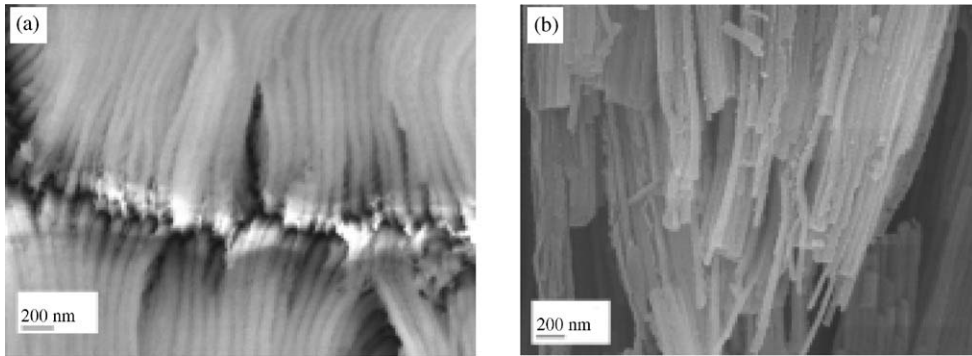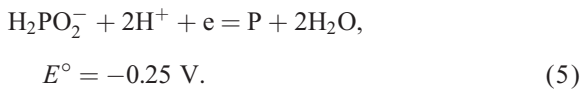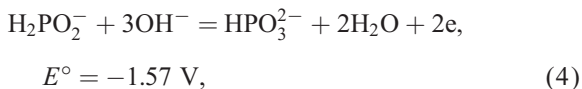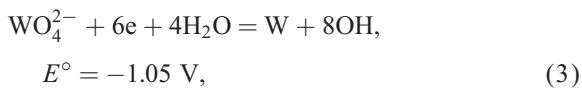$$Ni^{2+} + 2e = Ni, \quad E° = -0.25 \text{ V}, \qquad (2)$$
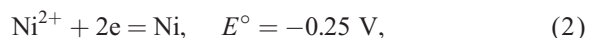
Fig. 1. SEM images of Ni–W–P nanowire arrays. (a) View from the top. (b) View from the side.

$$WO_4^{2-} + 6e + 4H_2O = W + 8OH,$$

$$E^\circ = -1.05 \text{ V}, \tag{3}$$

$$H_2PO_2^- + 3OH^- = HPO_3^{2-} + 2H_2O + 2e,$$

$$E^\circ = -1.57 \text{ V}, \tag{4}$$

$$H_2PO_2^- + 2H^+ + e = P + 2H_2O,$$

$$E^\circ = -0.25 \text{ V}. \tag{5}$$

The E° represents standard single electrode potential. If the E° value of a reductant is lower than that of an oxidizer, the reaction between an oxidizer and a reductant can take place in view of thermodynamics. The larger the electrode potential difference between an oxidizer and a reductant is, the higher the possibility of redox reaction is. According to the E° values, Ni, W and P could be reduced by NaH_2PO_2 in the electrolyte solution. However, these reactions among Eqs. (2)–(5) cannot take place without some catalyst, which is controlled by kinetics. Pd atoms act as a catalyst in the reactions. The growth mechanism of Ni–W–P nanowire arrays is as follows: first, $SnCl_2$ solution which is adhered to the pore wall of the AAM hydrolyzes formation $Sn(OH)_2$ in an aqueous solution, then, $PdCl_2$ is reduced to Pd atoms by $Sn(OH)_2$. Consequentially, these Pd atoms trigger the redox reactions. Once the redox reactions are triggered, the above reactions of Eqs. (2)–(5) can be autocatalyzed. In fact, as a catalyst, the concentration of Pd atoms is so low that no trace of it is seen on the EDS spectrum in Fig. 3. Since electroless deposition needs neither a supply of power nor a sprinkling of Au on one side of

the AAM before the deposition, and since these redox reactions are autocatalytic self-assembly processes and the electrolyte solution concentration is uniform, Ni–W–P nanowire arrays are formed where there is an electrolyte solution. The Ni–W–P nanowire arrays are definitely going to be large-scale and uniform (see Fig. 1 SEM images). The TEM and SAED images of single Ni–W–P nanowire are shown in Fig. 2. Fig. 2a shows that the Ni–W–P nanowire is about 60 nm in diameter and 3 µm in length. Fig. 2b illustrates that Ni–W–P nanowire is amorphous in structure, which is confirmed by the XRD spectrum as shown in Fig. 4. This amorphous structure of Ni–W–P nanowire arrays will meet the need of perpendicular anisotropy in magnetic properties. The EDS shown in Fig. 3 reveals that the nanowires are composed of Ni, W and P, the atomic ratio is 65.79:6.51:27.70, and the mass ratio is 65.28:20.22:14.50. Fig. 5 is the hysteresis loop of Ni–W–P nanowire arrays measured at room temperature. The $H_\parallel$ represents the external magnetic field parallel to the Ni–W–P nanowire arrays and the $H_\perp$ represents the external magnetic field perpendicular to the Ni–W–P nanowire arrays. As can be seen, the saturation magnetization (M_s) and remanence (M_r) of $H_\parallel$ are both larger than those of $H_\perp$. The $M_r/M_s(\parallel)$ is 0.61 and the $M_r/M_s(\perp)$ is 0.36. The coercivities (H_c) of Ni–W–P nanowire arrays for $H_\parallel$ and $H_\perp$ orientation are about 30000 and 32000 A m^{-1}, respectively. The hysteresis loops indicate that the easily magnetized direction of Ni–W–P nanowire arrays is parallel to the nanowire arrays and that it has obvious magnetic anisotropy. We can expect from Figs. 2b and
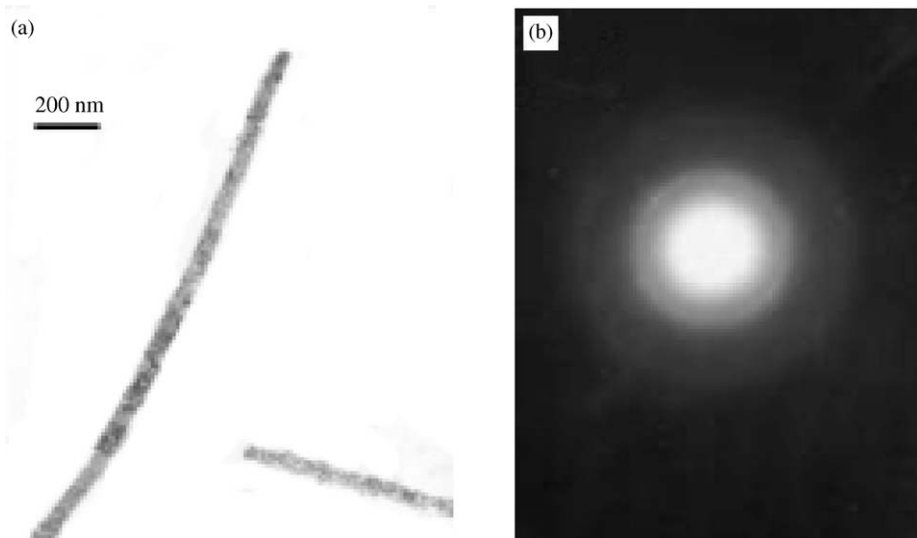
Fig. 2. (a) TEM image of Ni–W–P alloy nanowires with diameter about 60 nm. (b) SAED of Ni–W–P alloy nanowire.
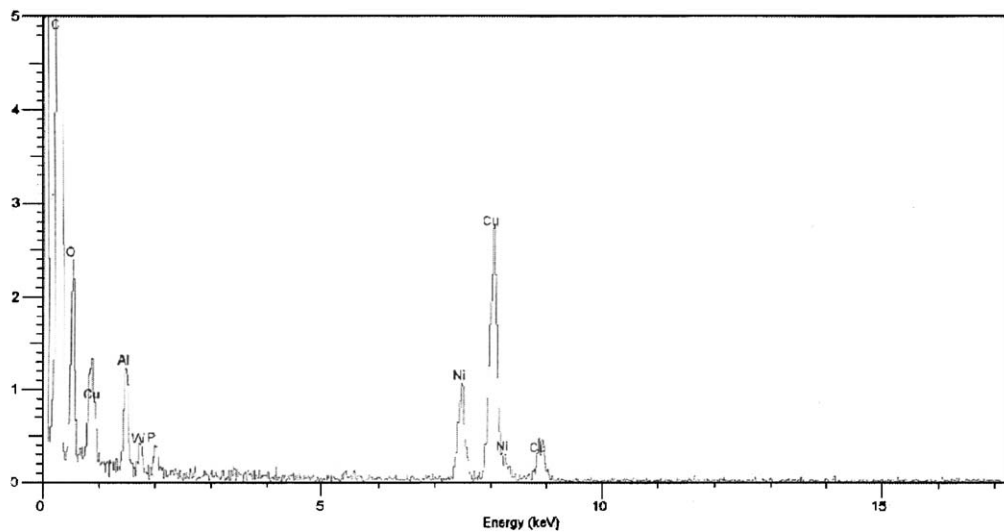

Fig. 3. The EDS of a Ni–W–P alloy nanowire. The atomic ratio of Ni:W:P is 65.79:6.51:27.70, the mass percentage of Ni:W:P is 65.28:20.22:14.50.

4 that the competition between shape anisotropy and magnetocrystalline anisotropy is unlikely to occur in the present case, because this latter contribution does not exist due to the amorphous structure of these Ni–W–P nanowires. The magnetic anisotropy of Ni–W–P nanowire is a result of the shape anisotropies.

It is due to the perpendicular anisotropy that the Ni–W–P nanowire arrays are a good candidate for ultra-high-density magnetic recoding media. The subject is therefore of interest in the field of magnetic nanostructure preparation and their associated anisotropy properties.
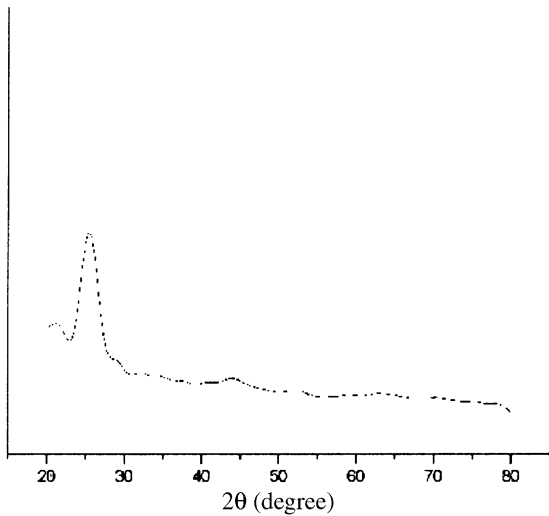
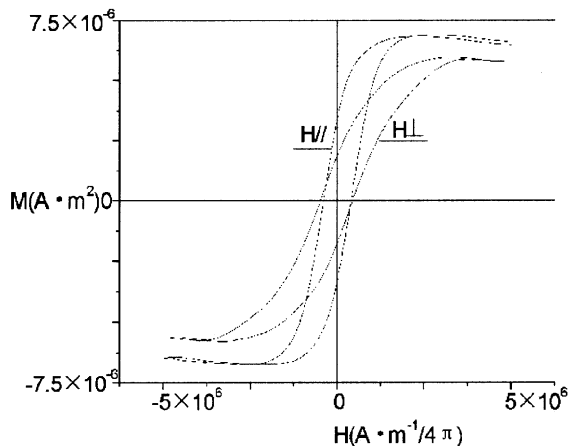Fig. 4. The X-ray diffraction pattern for Ni–W–P nanowires.

Fig. 5. Hysteresis loops of Ni–W–P nanowire arrays embedded in AAM at room temperature. The $H_{\parallel}$ represents the direction of magnetic field applied parallel to Ni–W–P nanowire arrays and the $H_{\perp}$ represents the direction of magnetic field applied perpendicular to Ni–W–P nanowire arrays.

4. Conclusions

Uniform size and shape of Ni–W–P magnetic nanowire arrays have been successfully fabricated on a large-scale by electroless deposition in AAM. The results indicate that the Ni–W–P nanowire is amorphous in structure. The hysteresis loops (Fig. 5) show that the easily magnetized direction of Ni–W–P nanowire arrays is parallel to the nanowire arrays and that it has obvious magnetic anisotropy as a result of the shape anisotropy. Electroless deposition method is an autocatalytic self-assembly process. It can be extended to many other materials and opens up significant opportunities in the nanoscale fabrication of magnetic materials for ultra-high-density magnetic recoding.

Acknowledgements

References

[1] H.R. Khan, K. Petrikowski, J. Magn. Magn. Mater. 215 (2000) 526.

[2] S.H. Ge, X. Ma, C. Li, W. Li, J. Magn. Magn. Mater. 226 (2001) 1867.

[3] K. Nieslch, F. Müller, A.P. Li, U. Gösele, Adv. Mater. 12 (2000) 582.

[4] W. Fritzsche, K.J. Böhm, E. Unger, J.M. Köhler, Appl. Phys. Lett. 75 (1999) 2854.

[5] S. Sun, C.B. Murray, D. Weller, L. Folks, A. Moser, Science 287 (2000) 1989.

[6] D. Routkevitch, A.A. Tager, J. Haruyama, D. Almawlawi, M. Moskovits, J.M. Xu, IEEE Trans. Electron Devices 43 (1996) 1646.

[7] P.L. Lu, S.H. Charap, IEEE Trans. Magn. 30 (1994) 4230.

[8] L. Piraux, S. Dubois, E. Ferain, J. Magn. Magn. Mater. 165 (1997) 352.

[9] P.M. Paulus, F. Luis, M. Kröll, G. Schmid, L.J. de Jongh, J. Magn. Magn. Mater. 224 (2001) 180.

[10] G.J. Strijkers, J.H.J. Dalderop, M.A.A. Broeksteeg, H.J.M. Swagten, W.J.M. deJonge, J. Appl. Phys. 86 (1999) 5141.

[11] S. Park, S. Kim, S. Lee, Z.G. Khim, K. Char, T. Hyeon, J. Am. Chem. Soc. 122 (2000) 8581.

[12] Y.W. Wang, G.W. Meng, C.H. Ling, G.Z. Wang, L.D. Zhang, Chem. Phys. Lett. 343 (2001) 174.

[13] S.G. Yang, H. Zhu, D.L. Yu, Z.Q. Jin, S.L. Tang, Y.W. Du, J. Magn. Magn. Mater. 222 (2000) 97.

[14] A.L. Prieto, M.S. Sander, M.S. Martin, R. Gronsky, T. Sands, A.M. Stacy, J. Am. Chem. Soc. 123 (2001) 7160.

[15] Y.W. Jun, S.M. Lee, N.J. Kang, J. Cheon, J. Am. Chem. Soc. 123 (2001) 5150.

[16] Y.W. Cao, R. Jin, C.A. Mirkin, J. Am. Chem. Soc. 123 (2001) 7961.

[17] F.K. Kim, J.H. Song, P.D. Yang, J. Am. Chem. Soc. 124 (2002) 14316.

[18] C.P. Gibson, K.J. Putzer, Science 267 (1995) 1338.

[19] M.P. Pileni, B.W. Ninham, T.G. Krzywicki, J. Tanori, I. Lisiecki, A. Filankembo, Adv. Mater. 11 (1999) 1358.

[20] M. Li, H. Schnablegger, S. Mann, Nature 402 (1999) 393.

[21] X. Peng, L. Manna, W. Yang, J. Wickham, E. Scher, A. Kadavanich, A.P. Alivisatos, Nature 404 (2000) 59.

[22] A. Brenner, G. Riddell, J. Res. Nat. Bur. Stand. 37 (1946) 1.

[23] H. Masuda, K. Fukuda, Science 268 (1995) 1466.